Medium Voltage Multilevel Converters for a Multi-MW Wind Turbine Grid Connection

Osman S. Senturk*, Lars Helle**, Stig Munk-Nielsen*, Pedro Rodriguez***, Remus Teodorescu*
*Aalborg University, Department of Energy Technology, Denmark
**Vestas Wind Systems, Denmark
***Universitat Politecnica de Catalunya, Spain

Abstract– Recent advances in the wind power technology have increased wind turbine power ratings to multi-MWs. This increase and recently introduced strict grid codes are spurring the utilization of full-scale medium voltage (MV) grid-side power electronics converters in wind turbines. In this study, for the grid connection of a hypothetical 6MW-3kV wind turbine, three-level (3L) configurations of NPC, FC, and HB VSCs are simulated for PF=0.9-1 and f_c=650-1050Hz. The simulation results show their performance with respect to total harmonic distortion of current, switch utilization, switch losses, and loss distribution. Finally, these VSCs are compared with respect to the two most important criteria (power density and reliability) for the 6 MW wind turbine connected to a MV (>3kV) grid via a transformer.

I. Introduction

Wind power penetration to electricity grids have been increased signifcantly in the recent decade. Therefore, more comprehensive grid codes for connection of wind power turbines to grids were needed and have been introduced recently. Meanwhile, the wind power technology has advanced as well such that wind turbine power ratings have exceeded 3MW [1]. These two advances have made utilization of full-scale grid side power electronics converters more practical such that these high performance converters can fulfill grid code requirements such as fault ride through and reactive power support. Practically, construction of these multi-MW converters in medium voltage levels rather than low voltage levels is advantageous due to fewer power electronics and control equipments, which affect power density, reliability, and cost of the converter [2]. Considering the aspects of power quality, semiconductor switch electrical and thermal stresses, and electromagnetic interference (EMI), multi-level (ML) voltage source converters (VSCs) are more promising than standard two-level VSCs for multi-MW MV applications [3]. In this study, three-level (3L) topologies of neutral point clamped (NPC), flying capacitor (FC), and H-Bridge (HB) as shown in Fig.1, 2, and 3 are chosen to be studied concerning power density and reliability, which are considered as the two most important criteria in wind turbine applications. As semiconductor switches of these converters, press-pack IGBTs with antiparallel diodes are chosen because of their high electrical ratings (e.g. 4.5kV-1.8kA-1kHz), small thermal resistance, snubber-free operation, etc. In this paper, 3L-NPC, -FC-, and -HB-VSCs with press-pack IGBT-diode pairs are simulated for a hypothetical 6MW-3kV wind turbine's grid connection via a transformer such that output waveforms and switch current waveforms demonstrate output power quality and switch utilization, respectively. Also, switch losses are calculated on-line by means of switch loss models based on a real IGBT press-pack device's parameters in order to compare power loss distribution over the converters. Then, the simulation results of these three VSCs are summarized. Finally, the VSCs are generally compared with respect to power density and reliability.

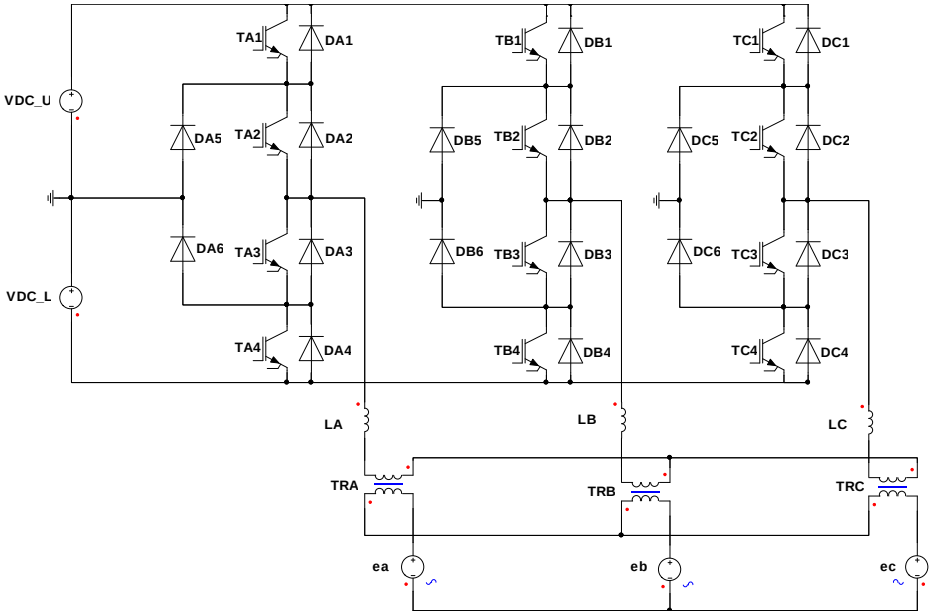

Fig.1. 3L-NPC-VSC power circuit.

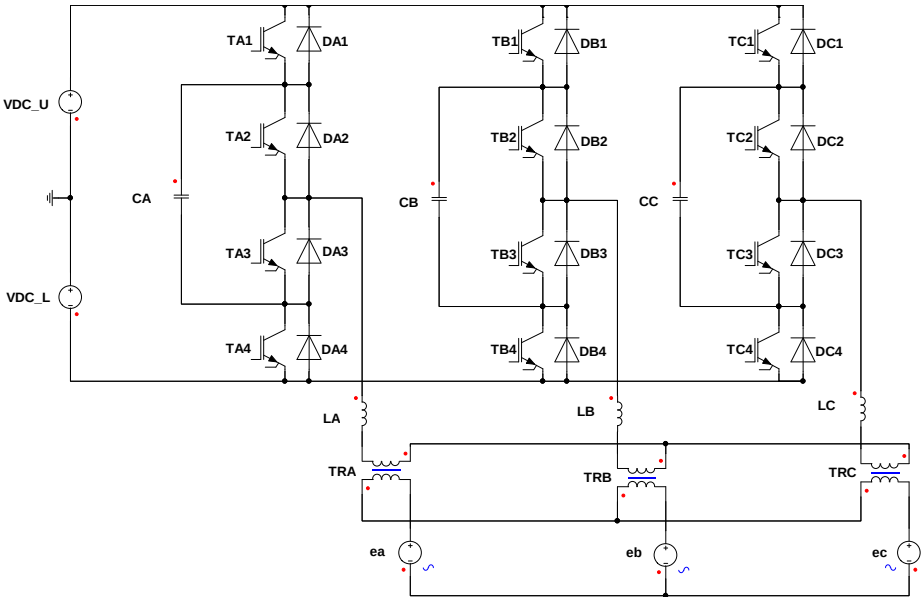

Fig.2. 3L-FC-VSC power circuit.

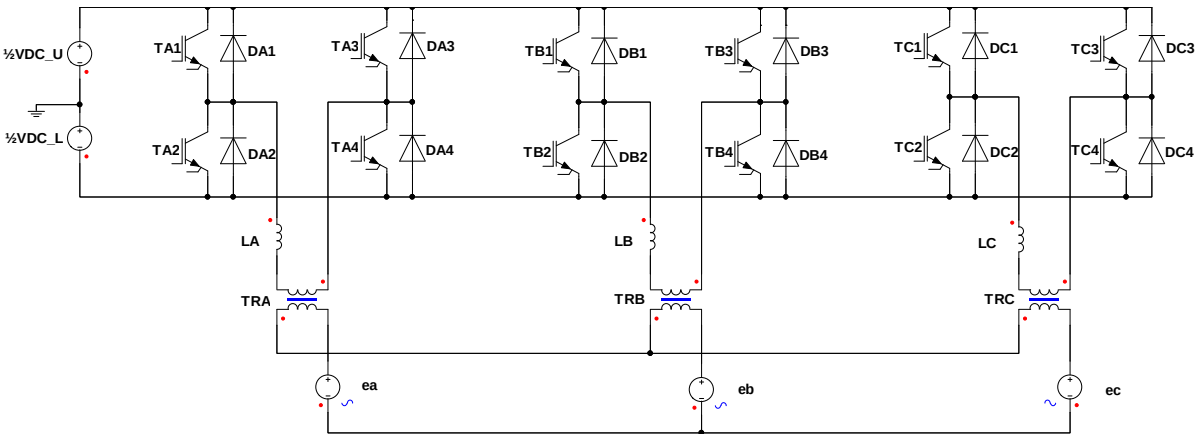

Fig.3. 3L-HB-VSC power circuit.

II. Simulation Models

The 3L-NPC-, -FC-, and -HB-VSCs are simulated by means of ideal components such as switches, voltage sources, capacitors, transformers, and inductors in Ansoft-Simplorer as seen in Fig.1, 2, and 3. The parameters of the simulation models are shown in Table I. In addition to electrically ideal switch models, power loss models of IGBTs and diodes are built based on a 4.5kV-1.8kA Westcode IGBT-diode pair (T1800GA45A) in order to calculate conduction, turn-on, and turn-off/reverse recovery losses on-line [4]. It should be noted that no switching ripple filter i.e. grid filter rather than a filter inductor is modeled because the study emphasizes on the converter itself. Likewise, neutral point balancing and flying capacitor voltage regulation are not considered in this study.

Table I. Simulation Parameters

	NPC	FC	HB
Output real power (P)	6MW	6MW	6MW
PF	0.9-1	0.9-1	0.9-1
Line-line output voltage (V_{LL})	3kV-50Hz	3kV-50Hz	3kV-50Hz
DC bus voltage (V_{DC})	2500+2500V	2500+2500V	2500V
Filter inductance (L)	450µH (10%)	450µH (10%)	450µH (10%)
Switching frequency (f_C)	650-1050 Hz	650-1050 Hz	650-1050 Hz
PWM	PD-PWM	PS-PWM	UPWM

In simulations, PF is limited to 0.9 considering grid code requirements. Switching frequency is limited by the maximum switching frequency of the IGBT and total harmonic distortion of the output current (THD_I). For the modulations of the converters, the most common carrier based PWM methods (with zero-sequence added reference output voltage signal) are utilized such that phase disposition PWM (PD-PWM) for NPC [5], phase shifted PWM (PS-PWM) for FC [6], and unipolar PWM (UPWM) [7] are realized.

III. Simulation Results

The outputs waveforms of each converter for PF=1 and f_c=1050Hz are shown in Fig.4, Fig.5, and Fig.6, through which it is observed that 3L-NPC-VSC supplies the output current with less ripple than 3L-FC-VSC and 3L-HB-VSC. The latter two converters supply almost the same output current. In Table II, THD_Is are summarized for each extreme PF and f_c condition.

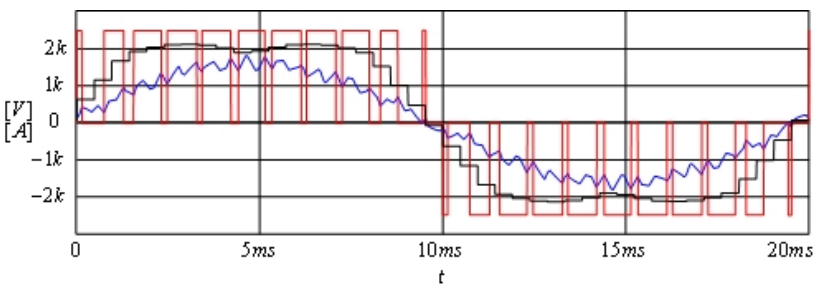

Fig.4. Output voltage reference (black), output voltage (red), and output current (blue) waveforms for 3L-NPC-VSC.

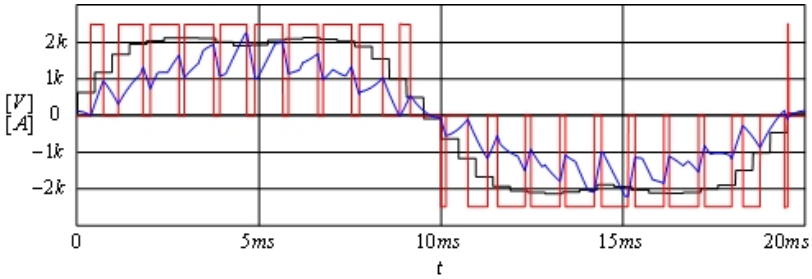

Fig.5. Output voltage reference (black), output voltage (red), and output current (blue) waveforms for 3L-FC-VSC.

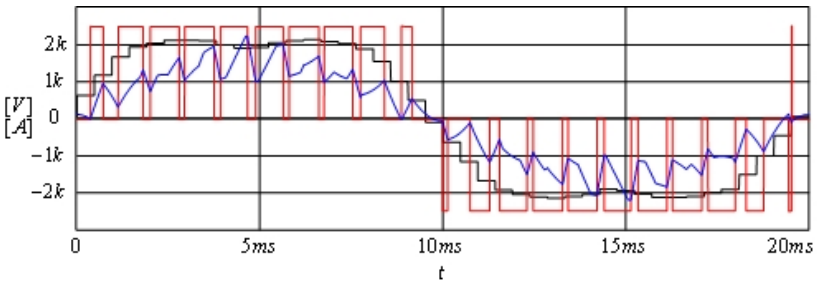

Fig.6. Output voltage reference (black), output voltage (red), and output current (blue) waveforms for 3L-HB-VSC.

Table II. Total Harmonic Distortion Comparison

THD_I (%)	f_c=1050 Hz		f_c=650 Hz	
	PF=1	PF=0.9	PF=1	PF=0.9
3L-NPC	8.8	8.1	14.2	13.4
3L-FC	20.9	17.4	34.2	28.8
3L-HB	21.0	17.3	34.1	28.7

Switch utilization in each converter for PF=1 and f_c=1050Hz are shown by each IGBT's and each diode's current waveforms in Fig.7, 8, and 9. It is obvious from the figures that 3L-NPC-VSC utilizes outer IGBTs and clamping diodes more extensively than 3L-FC- and 3L-HB-VSCs. However, the NPC does not utilize inner and outer diodes in this operation mode. Moreover, the utilization of these diodes is very insignificant even for PF=0.9.

On-line simulated conduction (P_{con}), turn-on (P_{on}), turn-off (P_{off}), and reverse recovery (P_{rec}) power losses of each IGBT and diode in each converter for PF=1 and f_c=1050Hz are shown in bar charts as seen in Fig.10, 11, and 12. In these charts, it is obviously seen that the outer IGBT of the NPC experience 30% more power loss than IGBTs of the FC and HB. Also, the FC and HB show very similar power loss pattern. Considering that IGBTs and diodes (except for clamping diodes) share the same press packs, IGBT-diode pair power losses are also important in the power loss distribution discussion and these losses are demonstrated in bar charts as seen in Fig.13, 14, and 15. It is noticed on these charts that the outer NPC switch pair and the switch pairs of the FC and HB experience almost the same power loss. In Table III, power loss distribution of each converter in each PF and f_c case is quantified by power loss deviation (ΔP_{loss}) term, which is defined in (1) where P_{avg} is the average power loss with respect to total number of IGBTs and diodes for switch-wise calculation or total number of IGBT-diode pairs for pair-wise calculation. The table shows that the IGBTs of the HB and FC converters show similar loss deviation and better loss distribution than the NPC IGBTs.

$$\Delta P_{loss}\ (\%) = 100*(|P_{loss}-P_{avg}|/P_{avg}) \qquad (1)$$

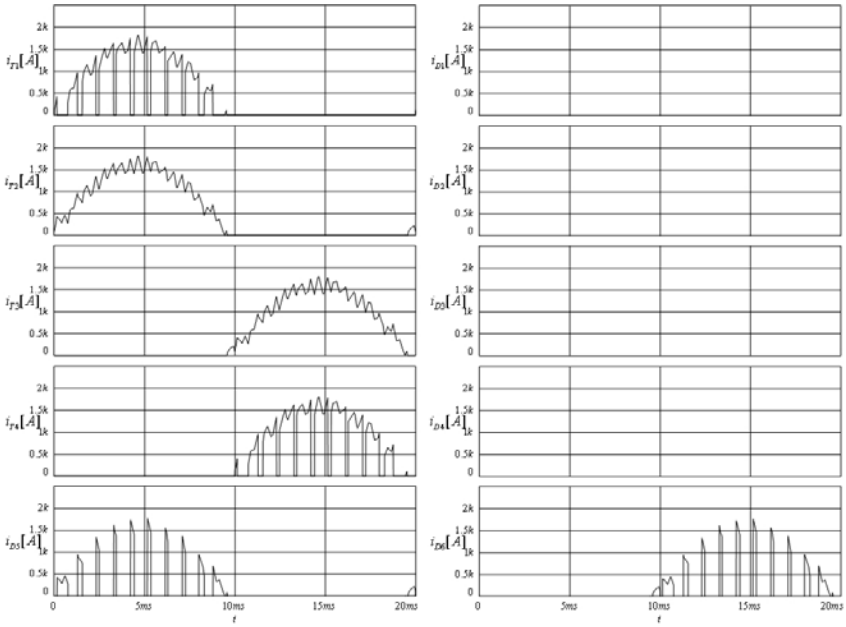

Fig.7. IGBT and diode current waveforms for 3L-NPC-VSC.

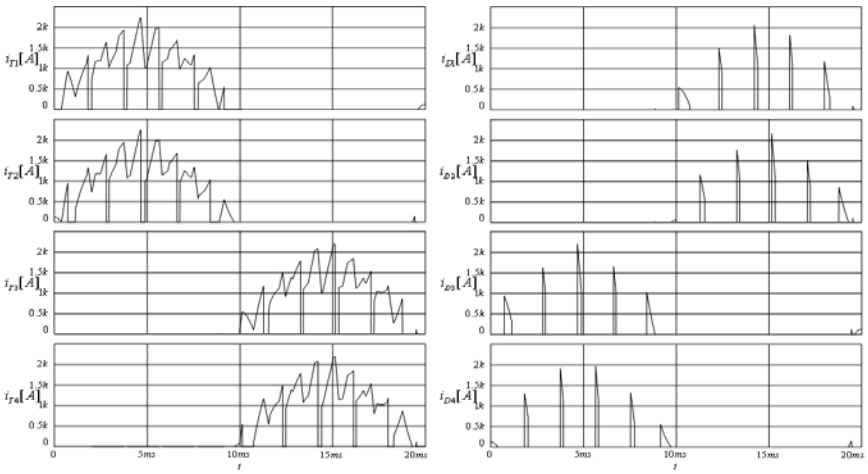

Fig.8. IGBT and diode current waveforms for 3L-FC-VSC.

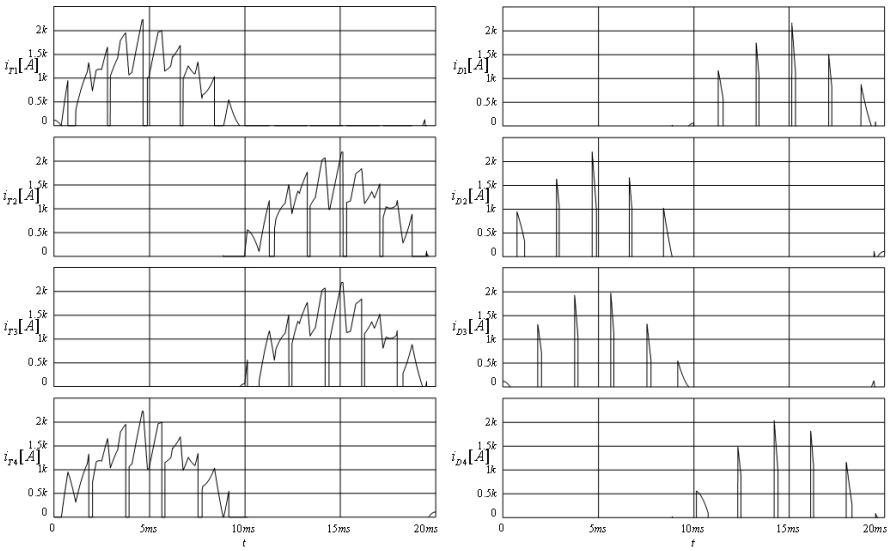

Fig.9. IGBT and diode current waveforms for 3L-HB-VSC.

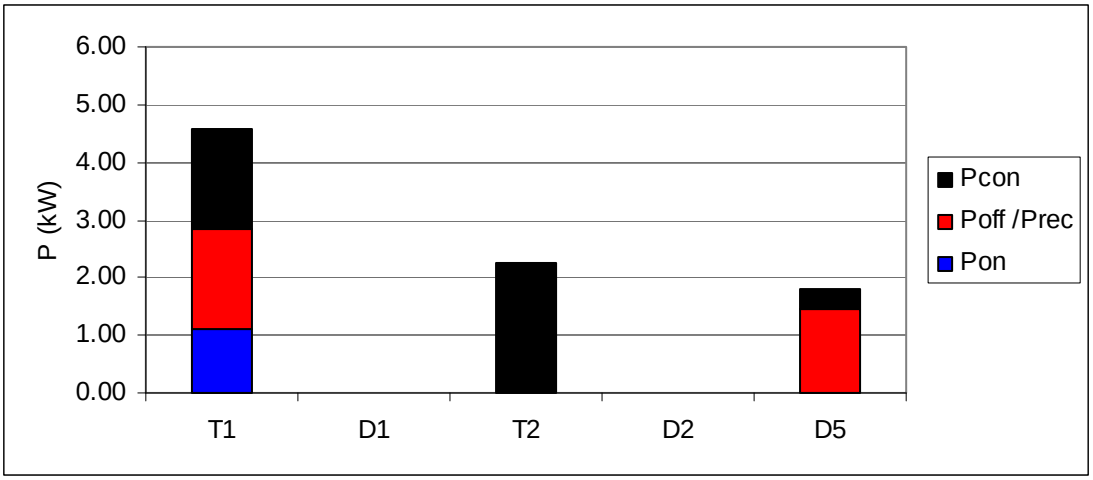

Fig.10. IGBT and diode power loss chart for 3L-NPC-VSC.

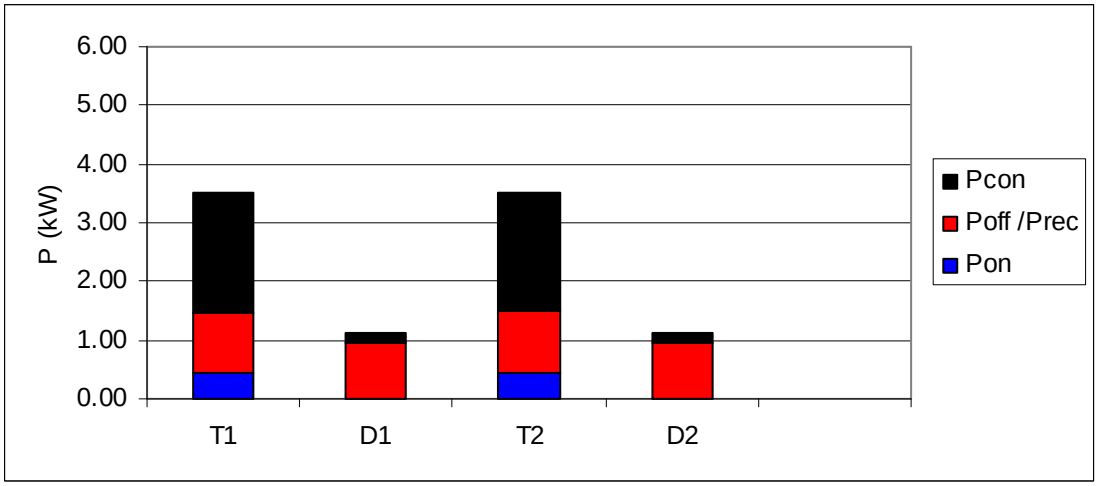

Fig.11. IGBT and diode power loss chart for 3L-FC-VSC.

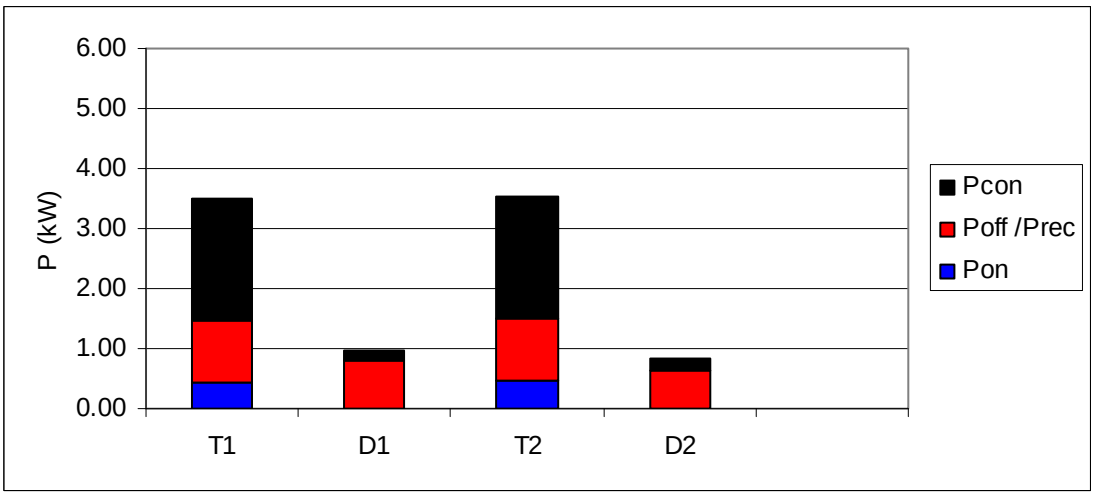

Fig.12. IGBT and diode power loss chart for 3L-HB-VSC.

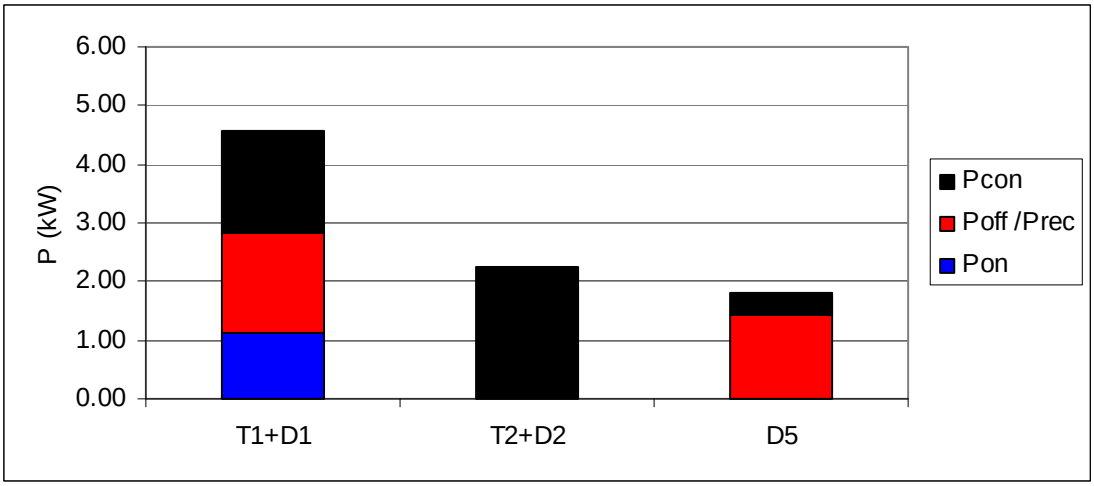

Fig.13. IGBT-diode pair power loss chart for 3L-NPC-VSC.

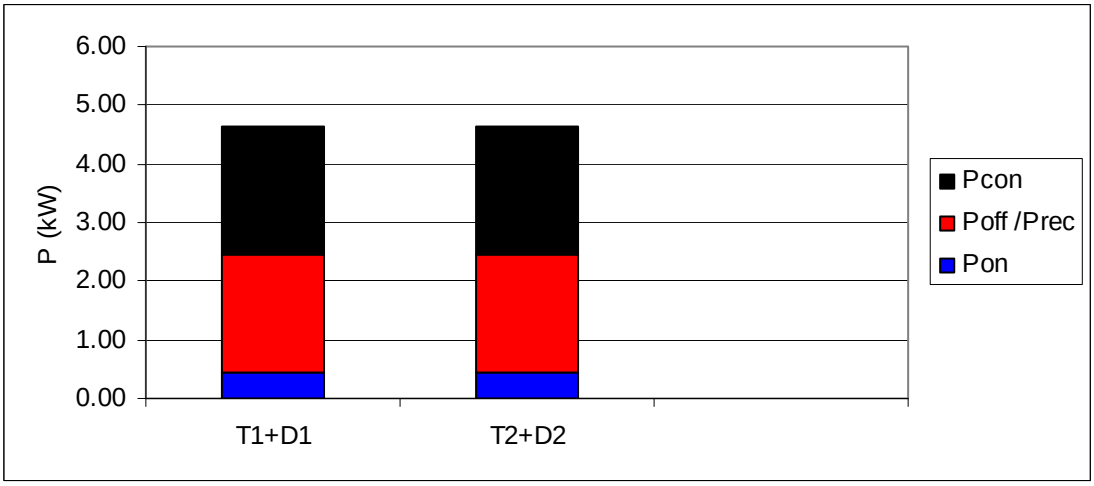

Fig.14. IGBT-diode pair power loss chart for 3L-FC-VSC.

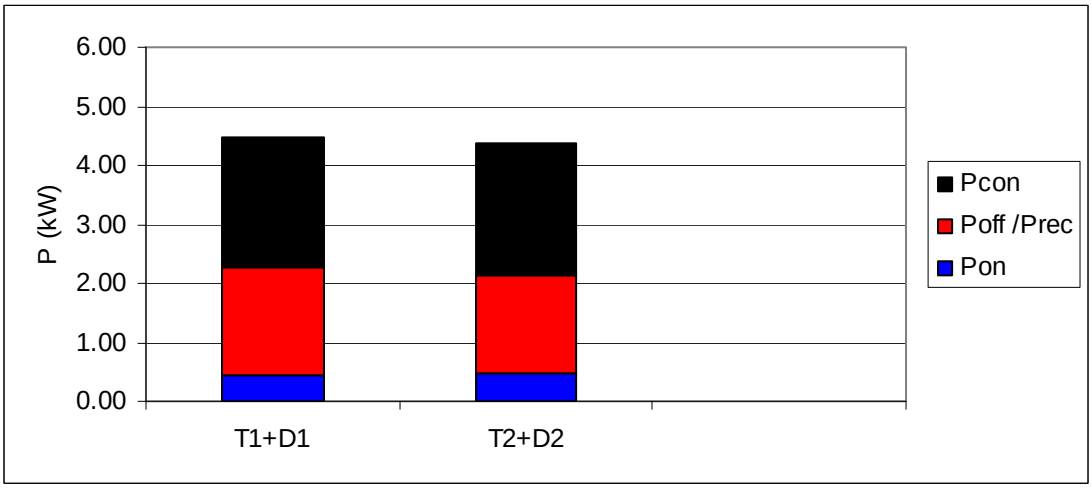

Fig.15. IGBT-diode pair power loss chart for 3L-HB-VSC.

Table III. Power loss deviation (ΔP_{loss})

ΔP_{loss} (%)	f_c=1050Hz & PF=1			f_c=1050Hz & PF=0.9		
	T1 / D1 / S1	T2 / D2 / S2	D5	T1 / D1 / S1	T2 / D2 / S2	D5
3L-NPC	165 / 100 / 59	30 / 100 / 21	4	156 / 91 / 59	40 / 99 / 15	5
3L-FC	50 / 50 / 0	50 / 50 / 0	-	57 / 57 / 0	57 / 57 / 0	-
3L-HB	57 / 55 / 1	60 / 62 / 1	-	61 / 63 / 0	66 / 64 / 0	-
ΔP_{loss} (%)	f_c=650Hz & PF=1			f_c=650Hz & PF=0.9		
	T1 / D1 / S1	T2 / D2 / S2	D5	T1 / D1 / S1	T2 / D2 / S2	D5
3L-NPC	146 / 100 / 47	60 / 100 / 4	6	152 / 100 / 51	71 / 100 / 3	22
3L-FC	58 / 57 / 0	59 / 59 / 0	-	79 / 80 / 0	80 / 79 / 0	-
3L-HB	64 / 64 / 1	63 / 63 / 1	-	68 / 65 / 2	62 / 65 / 2	-

IV. Conclusion

This study on grid connection of multi-MW wind turbines via MV power electronics converters compares the three well-known 3L-VSC topologies of NPC, FC, and HB by means of simulation results. Briefly, the NPC supplies higher quality output (two times better THD_I) than the FC and HB while the FC and HB show much better switch utilization and more equal power loss distribution. Moreover, it is observed that the effect of PF (within 0.9-1 range) is not significant on both THD_I and power loss distribution while f_c has strong effect on THD_I but not on power loss distribution.

V. Discussion

Two of the most important criteria in wind turbine applications are power density and reliability. The three converters studied via simulations in this paper can be generally compared with respect to these two criteria. Considering power density, the NPC requires smaller grid filter due to less THD_I than the others, however it has clamping diodes which increase the volume of the converter. Likewise, the FC has extra flying capacitors whereas the HB requires fewer DC capacitors than the FC and the NPC because it needs only the half DC bus voltage of the others. Considering reliability, the FC is the less advantageous because of its short lifetime flying capacitors while the NPC may more suffer from thermal cycling related lifetime due to its more thermally stressed outer switches. Also, the clamping diodes of the NPC add in the total number of components and in complexity; therefore, they can be considered as disadvantageous for reliability compared to the other converters.

References

[1] L. Helle, “Modeling and Comparison of Power Converters for Doubly Fed Induction Generators in Wind Turbines”, PhD Dissertation, Aalborg University, Aalborg, Denmark, 2007.

[2] A. Faulstich, J. K. Steinke, F. Wittwer, “Medium voltage converter for permanent magnet generators up to 5 MW,” in *Proc. Conf. Rec. EPE*, Dresden, Germany, 2005.

[3] B. Wu, *High-Power Converters and AC Drives*, Piscataway, NJ, IEEE Press, 2006.

[4] Westcode website: *www.westcode.com*

[5] D. G. Holmes, T. A. Lipo, *Pulse Width Modulation for Power Converters*, Piscataway, NJ, IEEE-Wiley, 2003.

[6] T. A. Meynard, H. Foch, P. Thomas, J. Courault, R. Jakob, M. Nahrstaedt, “Multicell converters: basic concepts and industry applications,” *IEEE Transactions on Ind. Electronics*, vol. 49, no. 5, pp. 955-964, 2002.

[7] N. Mohan, T. M. Undeland, W. P. Robbins, *Power Electronics Converters, Applications, and Design,* 4th Edition, John Wiley & Sons, 2003.